Experimental and numerical evaluation of friction stirs welding of AA 2024-W aluminum alloy

Dr.Ayad M. Takhakh
ayadmurad@nahrainuniv.edu.iq

Hamzah N. Shakir
almohands4ever@gmail.com

Abstract

Friction Stir Welding (FSW) is one of the most effective solid states joining process and has numerous potential applications in many industries. A FSW numerical tool, based on ANSYS F.E software, has been developed. The amount of the heat gone to the tool dictates the life of the tool and the capability of the tool to produce a good processed zone. Hence, understanding the heat transfer aspect of the friction stir welding is extremely important for improving the process. Many research works were carried out to simulate the friction stir welding using various softwares to determine the temperature distribution for a given set of welding conditions. The objective of this research is to develop a finite element simulation of friction stir welding of AA2024-W Aluminium alloy. Numerical simulations are developed for thermal conductivity, specific heat and density to know the relationship of these factors with peak temperature. Variation of temperature with input parameters is observed. The simulation model is tested with experimental results. The results of the simulation are in good agreement with that of experimental results.

الحلول العملية والرقمية للحام الاحتكاكي بالمزج (FSW) لسبيكة المنيوم AA2024-W

أ.م.د. أياد مراد طخاخ **م. حمزة نورالدين شاكر**

جامعة النهرين / كلية الهندسة

الخلاصة

يعد اللحام الاحتكاكي بالمزج (FSW) واحد من الطرق الفعالة للحام الحالة الصلبة ويدخل في الكثير من التطبيقات في مختلف الصناعات . تم تطوير حلول رقمية للحام الاحتكاكي بالمزج بالاعتماد علر برنامج ANSYS لحساب كمية الحرارة المتولدة خلال عملية اللحام والتي تؤثر على عمر وجودة منطقة اللحام والعدة، اذ ان من المهم معرفة كيفية انتقال الحرارة خلال اللحام الاحتكاكي بالمزج. عدد من الباحثين درسو توزيع درجات الحرارة خلال هذا النوع من اللحام باستخدام برامجيات متعددة. الغرض من هذا البحث تطوير حلول رقمية باستخدام طريقة العناصر المحددة (FEM) بالاستناد على برنامج ANSYS لسبيكة المنيوم نوع AA2024-W . تم تطوير هذه الحلول بالاعتماد على العلاقة التي تربط خواص التوصيل الحراري و الحرارة النوعية و الكثافة مع درجات الحرارة حيث تتغير هذه الخواص بتغير درجات الحرارة. المحاكة التي تم الحصول عليها تم التحقق عملياً من نتائجها واظهرت نتائج المقارنة وجود توافق جيد .

Keywords: Friction stir welding, AA 2024-W, Temperature distribution, Simulation.

Introduction

A method of solid phase welding, which permits a wide range of parts and geometries to be welded and called friction stir welding (FSW), was invented by W. Thomas and his colleagues of The Welding Institute (TWI), UK, in 1991. Friction stir welding can be used for joining many types of material and metal combinations, if tool material and designs can be found which operate at the forging temperature of the workpieces. The process has been used for manufacture of butt welds, overlap welds, T-sections and corner welds. For each of these joint geometries specific tool designs are required which are being further developed and optimized [1,2]. Friction stir welding is a relatively simple process as shown in Fig. 1.

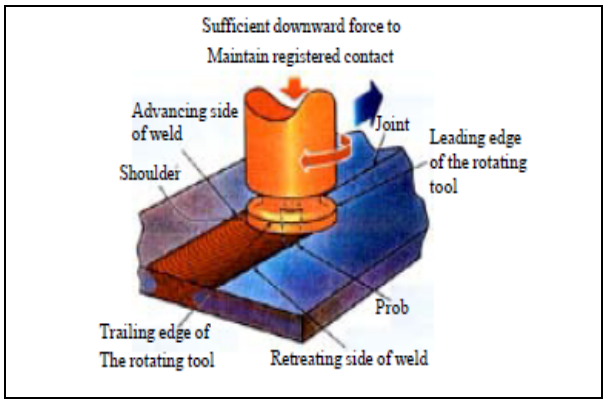

Fig.1: Schematic diagram of FSW process [1].

This process has been widely used in many industries such as space, aircraft, marine, transport and food processing. Low distortion, high quality, lower residual stresses, fewer weld defects and low cost joints are the main advantages of this method [3]. Friction stir welding (FSW) is a solid-state joining process in which a rotating tool,

consisting of a shoulder and a (generally threaded) pin, moves along the butting surfaces of two rigidly clamped plates placed on a backing plate. The shoulder is in sustained contact with the top surface of the workpiece. Part of the heat is generated by the friction between the shoulder and the workpiece, and another part is generated by material stirring. This heat softens the material to be welded. Severe plastic deformation and flow of this plasticised metal occurs as the tool is translated along the welding direction. A FSW joint consists of various zones involving different microstructures and mechanical properties. The heat affected zone (HAZ) is the most distant from the joint centerline. It is not deformed during the process, but the microstructure evolves due to the welding thermal cycles, influencing the mechanical properties. The thermomechanically affected zone (TMAZ) and the weld nugget are highly deformed by the material rotational flow [4]. Due to the interesting features of
FSW, lots of research activities have been carried out on different materials (aluminum alloys first of all, but also steel, titanium, magnesium, copper, polymers etc.) and on different weld geometries [5].
Consequently, numerical simulation could be a helpful device for predicting process behavior and its optimization .In friction stir welding, heat is generated first on the basis of friction between tool and work piece and then by shape change. A

portion of the generated heat disseminated through work piece, will affect distortion, residual stress distribution as well as weld quality of the during welding process, but also can save research time and cost [7]. Some studies of FSW on temperature field and residual stresses have been carried out through FEM software i. e. ANSYS® [8-9], ABAQUS [10-13], Forge® [14], DEFORM-3D™[15]. Finite element Methods also used to study the effect of FSW process parameters on mechanical properties of various welded alloys based on solid mechanics [16] or develop the mathematical model. [17].

Thus, much research has been done to study the simulation of temperature distribution during friction stir welding process. This was recognized in present study based on ANSYS software, the results obtained for simulation was comparison with that actual experiment.

piece [6]. Finite element analysis is an effective method in the investigation of welding, because it not only can obtain the instantaneous results

Experimental work

Friction stir welds were made on the plate samples of 2024-Waluminum alloy on –W treatment which used to describe an as quench condition between solution heat treatment and artificial or room temperature aging.

The test plates of size 200 mm X 100 mm X 3.5 mm are prepared from aluminum alloy AA2024 plates Fig.2. The chemical composition and mechanical properties of the base material are presented in Table 1 and Table 2, respectively. The experiment is conducted using FSW machine developed by TAKSAN milling machine, as shown in Fig.3.The welding was done by single pass.

Table 1: Chemical composition of Al 2024-W alloy.

Element	Zn	Cu	Fe	Ni	Mn	Ti	Si	Mg	Cr	Al
Weight %measured	0.06	3.87	0.3	0.02	0.38	0.005	0.16	1.39	0.006	93.83
Standard [24]	-	4.4	-	-	-	-	0.18	1.5	-	-

Table 2: Typical mechanical properties of wrought aluminum 2024-W alloy.

	Ultimate strength(MPa)	Yield strength(MPa)	Percentage of elongation	Hardness HV
Measured	365	-	22%	105
Standard [25]	335		28%	110

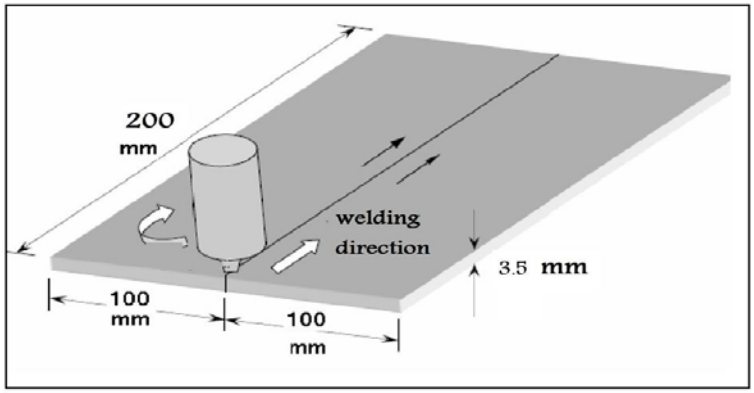

Fig 2 :Dimensions of welded plate

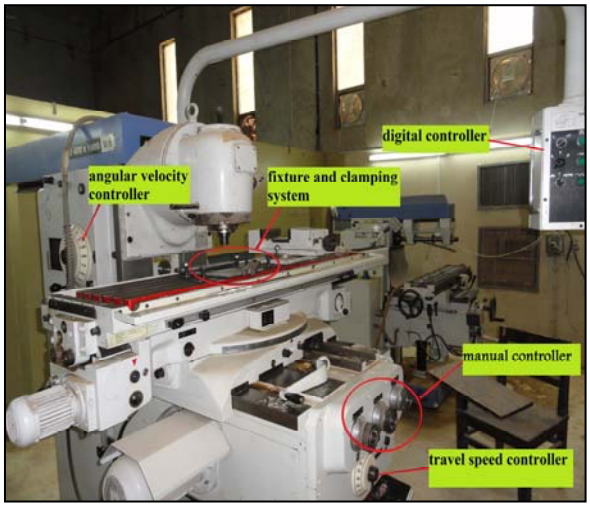

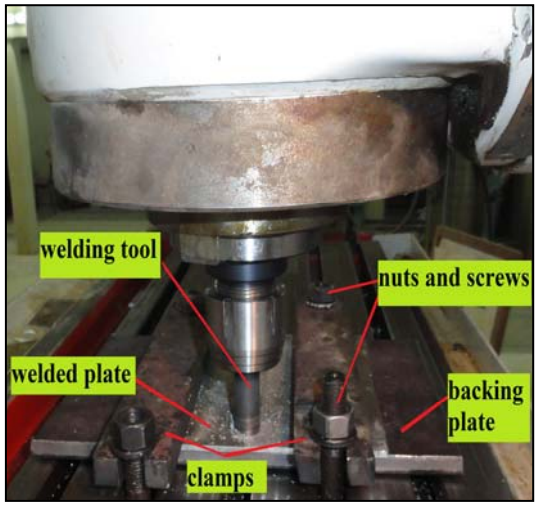

Fig. 3: Taksan milling machine

The FSW tools are manufactured using Turning machine. The configuration of the designed FSW Tool is:

• Tool pin profile of cylindrical without draft.

• Tools having ratio of shoulder diameter to pin diameter(D/d) is 3 has been chosen for this study because it is having good joining properties among various pin configurations [17].The manufactured tool is shown in Fig. 4.

The research work was planned to be carried out in the following steps:

1. Identifying the important process parameter

2. Finding the upper and lower limits of the process parameter Viz. tool rotational speed and welding speed to select the best result of welding efficiency for simulation.

3. Checking the adequacy of the numerical simulation.

4. Conducting the conformity test runs and comparing the results.

Fig. 4: FSW Tool (X38 tool steel)

To determine the tensile strength of the stir zone, tensile test specimens were sectioned as per ASTM E8 in the transverse direction perpendicular to the weld line with CNC milling machine as shown in Fig.5. Transverse tensile tests were performed on PHYWE machine to evaluate the mechanical properties of the joints.

FSW parameters used in this study were listed in Table 3. The rotating tool used in this study was made of X38 tool steel.

FSW parameters used in this study were listed in Table 3. The rotating tool used in this study was made of X38 tool steel.

Table 3: FSW work parameters

Sample No.	Welding speed(mm/min)	Rotation speed(rpm)
F1	20	900
F2	30	900
F3	40	900
F4	20	710
F5	30	710
F6	40	710

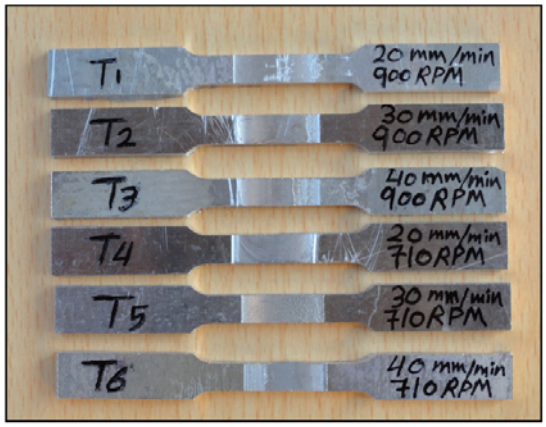

Fig. 5: Tensile specimens before test.

Thermal Modeling of FSW

FEM is most commonly used in numerical analysis for obtaining approximate solutions to wide variety of engineering problems. In the present study, a commercial general purpose finite element program ANSYS® 11.0 was used for numerical simulation of friction stir welding process. The ANSYS® program has many finite element analysis capabilities, ranging from simple, linear, static analysis to a complex nonlinear, transient dynamic analysis. The thermal and mechanical responses of the material during friction stir welding process are investigated by finite element simulations.

In this study, a thermal model is developed for analysis. First, brick element is SOLID70, Homogenous; a linear, transient three-dimensional heat transfer model is developed to determine the temperature fields, rate independent. The finite element models are parametrically built using APDL (ANSYS Parametric Design Language) provided by ANSYS® [18]. The model are then validate by comparing the results with established material data

Mathematical thermal model.

Simple analytical solution to the heat flow problem can be found. Instead, a numerical solution is sought, based on a descretization of Fourier's 2nd Law:

$$\rho c \frac{\partial T}{\partial t} = \lambda \left(\frac{\partial^2 T}{\partial x^2} + \frac{\partial^2 T}{\partial y^2} + \frac{\partial^2 T}{\partial z^2} \right) + \frac{q_0}{V} \qquad (1)$$

Where ρc is the volume heat capacity, λ is thermal conductivity, *x*, *y*, and *z* are the flow simulations space coordinates; and q_0 /*V* is the source term [19].

Assumptions.

The following assumptions are made in developing the model;

- The heat generation is due to friction and Heat generated during penetration and extraction is also considered.
- The coefficient of friction is considered changed and dropped with increasing temperature.
- Material properties are uniform.
- Heat transfer from the workpiece to the clamp is negligible [18].

The important process characteristics which are required to be considered for the purpose of modeling are as follows:

a) Moving heat source;

b) Weld speed.

c) Axial load to calculate heat generation.

d) Material properties.

Elements Used

In the present thermal analysis, the workpiece is meshed using a brick element called SOLID70. This element has a three-dimension thermal conduction capability and can be used for a three-dimensional, steady-state or transient thermal analysis. The element is defined by eight nodes with temperature as single degree of freedom at each node and by the orthotropic material properties. Heat fluxes or convections can be input as surface loads at the element faces as shown on the two faces in Figure 8. An advantage of using this element is that, the element can be replaced by an equivalent structural element for the structural analysis.

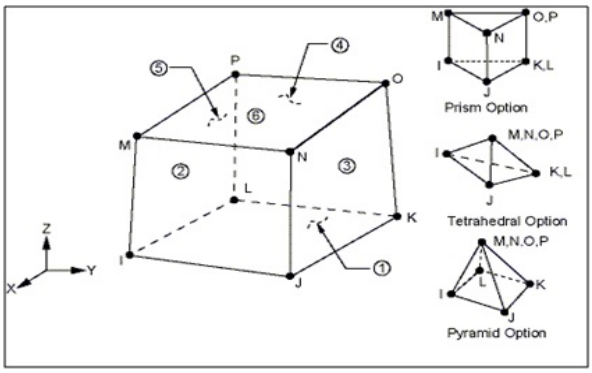

Fig. 6: three dimensional thermal solid elements SOLID70 [18]

As SOLID70 cannot apply heat flux and convection at the same time, a three-dimensional thermal-surface-effect element was used. For applying convection on the workpiece surface, SURF152 was used overlaying it onto faces of the base elements made by SOLID70. The convections were applied as a surface load by choosing KEYOPT. Figure 6 shows the geometry, node locations, and the coordinate system of the element, which is defined by four to nine nodes and the material properties [18].

Mesh Development

Three dimensional SOLID70 elements were used to mesh the sheets. The workpiece was divided into small parts along the length and along the width as shown in figure below.

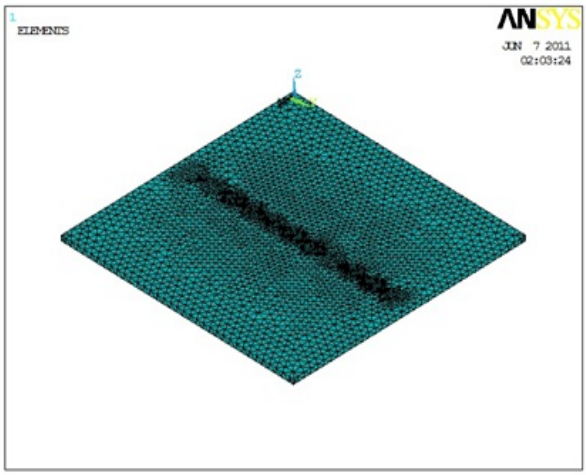

Fig. 7: 3D mesh of modeled welded plates for aluminume alloy in ANSYS program

Material Properties

Thermal properties of the material such as thermal conductivity, specific heat, and density are temperature dependent. An accurate estimation of temperatures is critical in FSW process because the stresses and strains developed in the weld are temperature dependent. Therefore, temperature dependent thermal properties of 2024 Aluminum alloy are used in finite element model. The thermal material properties of 2024 Aluminum alloy are tabulated in Table 4.The thermal property values are obtained from ref. [20], and for higher temperatures the values are linearly extrapolated.

Table 4 Thermal material properties of 2024 Aluminum alloy.[20]

T °C	Density kg m^{-3}	C_p J K^{-1} g^{-1}	H_T-H_{25} Jg^{-1}	λ Wm^{-1} K^{-1}
25	2785	0.85	0	175
100	2770	0.90	66	185
200	2750	[0.95][c]	159	193
300	2730	0.97	255	193
400	2707	1.00	353	190
500	2683	1.08	457	188
538[a]	2674	1.10	566	188
632	2500	1.14[c]	970	85.5
700	2480	1.14[c]	1048	85
800	2452	1.14[c]	1162	84

Boundary Condition

Boundary condition for FSW thermal model were specified as surface loads through ANSYS® codes. Assumptions were made for various boundary conditions based on data collected from various published research papers.

Convective and radiative heat losses to the ambient occurs across all free surfaces of the workpiece and conduction losses occur from the workpiece bottom surface to the backing plate. To consider convection and radiation on all workpiece surfaces except for the bottom, the heatloss qs is calculated by equation (2). [18]

$$q_s = \beta(T - T_0) + \epsilon\sigma(T^4 - T_0^4) \qquad (2)$$

where T is absolute temperature of the workpiece, T_o is the ambient temperature, β is the convection coefficient, ε is the emissivity of the plate surfaces, and σ = 5.67 x 10^{-12} $w/m^2.°C$ is the Stefan-Boltzmann constant. In the current model, a typical value of β was taken to be 10 $w/m^2.°C$ using an ambient temperature of 25C^0.

In order to account for the conductive heat loss through the bottom surface of weld plates, a high overall heat transfer coefficient has been assumed. This assumption is based on the previous studies. The heat loss was modeled approximately by using heat flux loss by convection q_b given by equation (3). [18].

$$q_b = \beta_b(T - T_0) \qquad (3)$$

where β_b is a fictitious convection coefficient.Due to the complexity involved in estimating the contact condition between the sheet and the

backing plate, the value of β_b had to be estimated by assuming different values through reverse analysis approach. In this study, the optimized value of β_b was found to be 100 [$18 w/m^2 . ^{\circ}C$

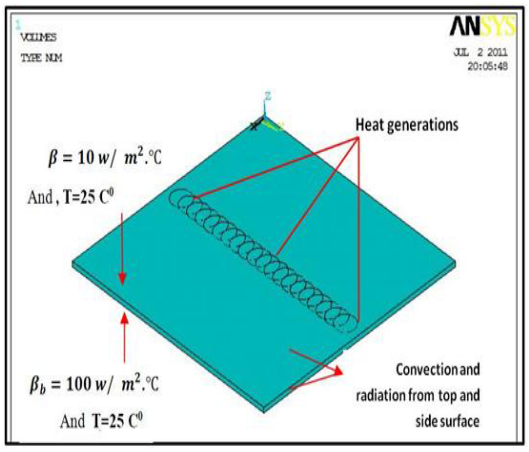

Fig. 8: Schematic representation of boundary condition for thermal analysis.

Heat Generation input during FSW.

For the ideal case considered, the torque required to rotate a circular shaft relative to the plate surface under the action of an axial load is given by [19]:

$$q_o = \int_0^{M_R} dM = \int_0^{R} \mu P(r)\, 2\pi r^2\, dr = \frac{2}{3}\mu \pi P R^3 \qquad (4)$$

Where M is the interfacial torque, μ is the friction coefficient, R is the surfac e radius, and $P(r)$ is the pressure distribution across the interface (here assumed constant and equal to P). If all the shearing work at the interface is converted into frictional heat, the average heat input per unit area and time becomes

$$q_o = \int_0^{M_R} \omega\, dM = \int_0^{R} \omega\, 2\pi \mu P r^2\, dr \qquad (5)$$

where q_0 is the net power (in Watts) and ω is the angular velocity (in rad/s). The next step is to express the angular velocity in terms of the rotational speed N (in rot/s). By substituting ω = 2πN into Eq. (5), we get

$$q_o = \int_0^{R} 4\pi^2 \mu P N r^2\, dr = \frac{4}{3}\pi^2 \mu P N R^3 \qquad (6)$$

From Eq. (6), it is obvious that the heat input depends both on the applied rotational speed and the shoulder radius, leading to a nonuniform heat generation during welding. These parameters are the main process variables in FSW [19].

From equation (6) we can get the heat generation by divide the net power q_0 on the volume of shoulder[19]:

$$Q_{sh} = \frac{q_o}{V_{sh}} \qquad watt/m^3 \qquad (7)$$

Where $V_{sh} = A_{sh} * t$, where V_{sh} is the shoulder volume, A_{sh} is the area of shoulder, t is the thickness.

$$A_{sh} = \pi * R_{sh}^2$$

Where the coefficient of friction of aluminum is 0.4 [19 , 21], this value is changed and dropped gradually in friction stir welding because the coefficient of friction μ varies with temperature and reached to 0.3 [22].where The temperature measurement in FSW for the workpiece was reported that the maximum temperature developed during FSW process ranges from 80% to 90% from melting temperature of the welding material [20].

Simulation

The thermal modeling was carried out. Transient thermal analysis is the stage. Figure 9 illustrates the flow diagram of the method used for the finite element analysis.

In order to simplify the moving tool on the sheet welded line in ANSYS program , all next steps (as shown in flow chart) was made to make it likemoving tool along welded line in the ANSYS program.

To get a good accurate of results, more steps of shoulder area must make in the simulation of program as shown in figure 10

.

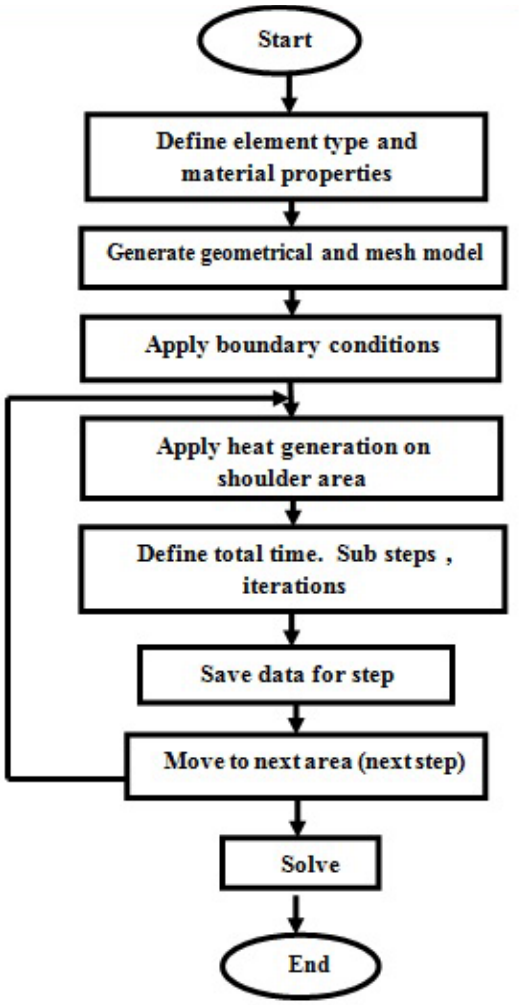

Fig. 9: Flowchart of thermal modeling.

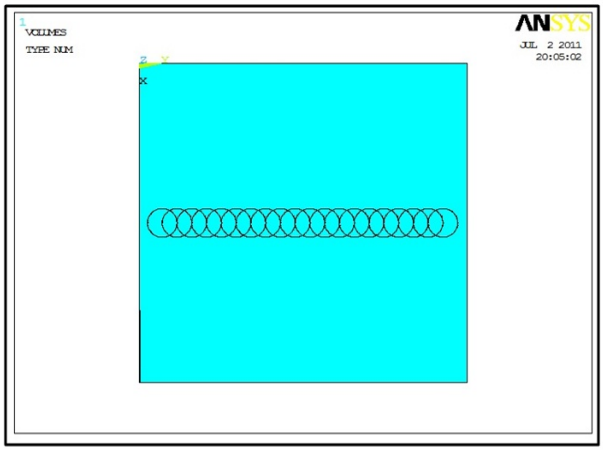

Figure 10: steps of circular shoulder area along welded line.

here each shoulder circle has heat generation and time step, also each circle represents one step.

Heat input (heat generation) is estimated by trial and error from ANSYS program because applied pressure P from equation 4 is unknown.

The method of heat input calculation by trial and error found by take the data (temperature and time) of thermocouple readings for one point (for example A in fig. 11) where in these data we depend on maximum temperature and make the following steps:

1- Assumed high value of heat generation where this value entered in program to make simulation for aluminum plate to get the maximum temperature at point *A*.
2- Assume low value of heat generation and examined it in program by make simulation for the aluminum plate at point *A* to get maximum temperature for these low value of heat generation.
3- Applying the interpolation on these (three values of temperature and two values of heat generation) to get a good agreement heat for this work .

After get good agreement heat generation, applying it in other steps of program.

From the validation shows that the present work can be used for modeling thermal distribution.

Four K-type thermocouples at selected points of aluminum sheet as shown in figure 11 have been used for measuring the temperature distribution by using temperature recorder type BTM-4208SD which contains 12 channels as shown in figure 11 (a &b) when these four thermocouples have been embedded in selected positions to 1.5 mm on the aluminum sheet as shown in figure (12 left) where recorded data temperatures changed with time are saved as excel file in the RAM of temperature recorder as shown in figure (12. right).

Fig. 11.a , Temperature recorder

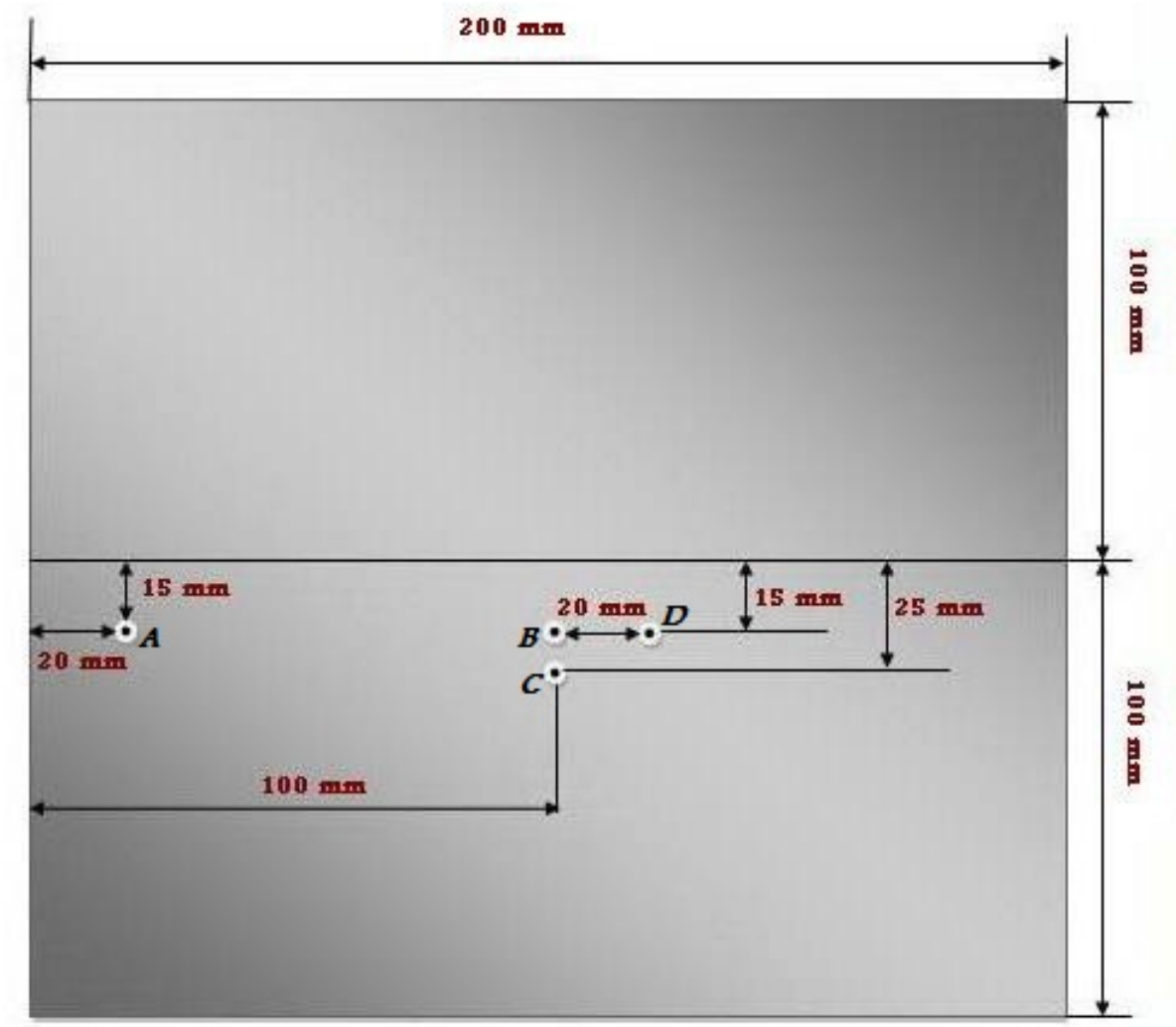

Fig. 11.b :Thermocouples location embedded on aluminum workpiece.

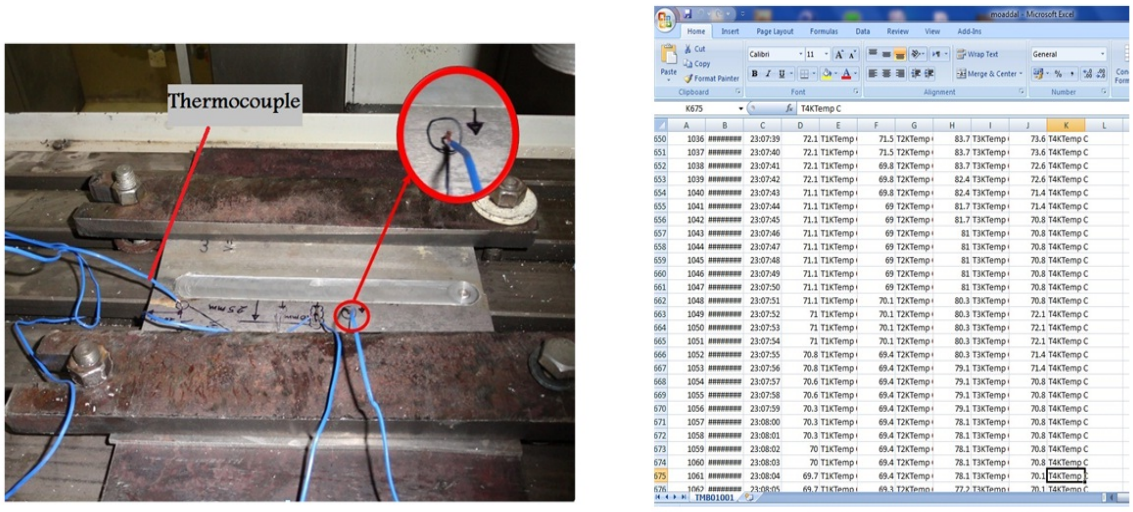

Fig. 12: Thermocouples embedded in the aluminum plate (left), Temperatures data as Excel file (right).

Results and discussions

The employed model may be utilized to predict temperature distribution during FSW operations under working conditions. Figures (17 to 24) shows the temperature distributions in the workpiece welded with rotational speed 710 rpm and welding velocity 40mm/min ,which has the best tensile properties of the weldments are given in Table 3. The weld strength is about 86% of that of AA 2024 base metal strength in W condition. All the tensile testing specimens were fractured in the stir zones of the welds.

Experimental results friction stir welding of material 2024 Al alloy were compared with simulation results of ANSYS program. The welded workpiece had dimensions 200 × 200 × 3.5 mm, the tool had a shoulder radius of 9 mm, pin radius of 3 mm and pin length of 3.3 mm. the rotation speed and translational speed that utilized in this comparison were 710 *RPM* and 40 *mm /min* respectively.

Figures below 13 to 16 show the results that calculated experimentally and simulation

:

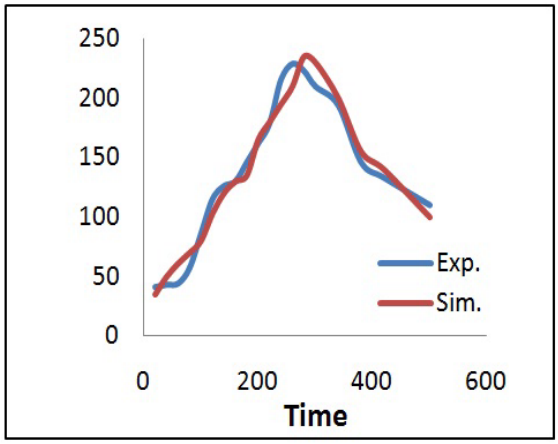

Fig. 13 : Temperature distribution in point $\omega = 710$ RPM , $v = 40$ mm/minA.

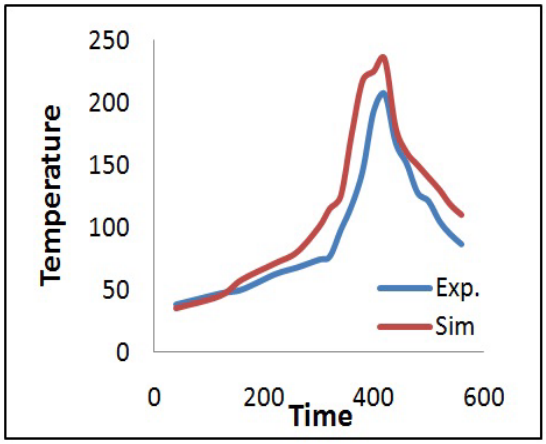

Fig. 14 : Temperature distribution in point $\omega = 710$ RPM , $v = 40$ mm/minB .

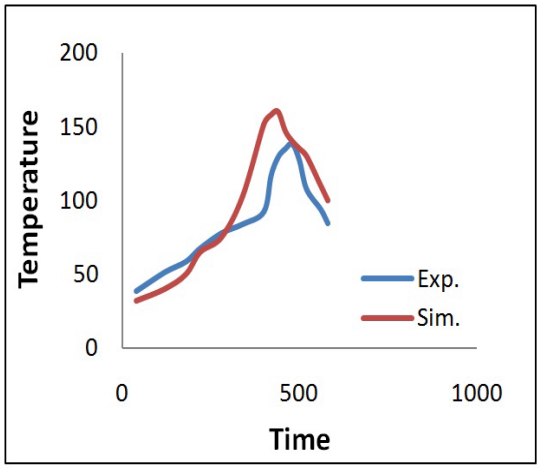

Fig. 15: Temperature distribution in point C. $\omega = 710\ \text{RPM}, v = 40\ \text{mm/min}$

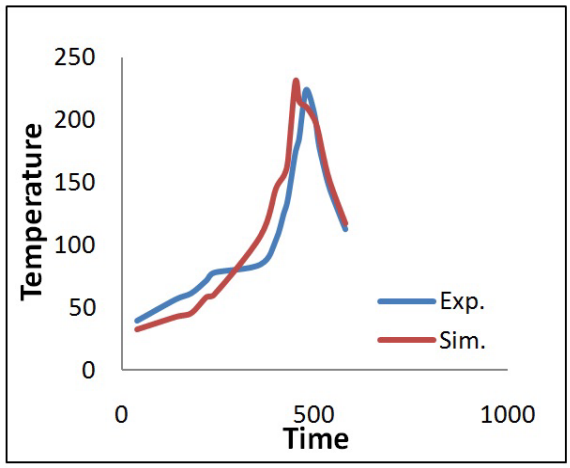

Fig. 16 : Temperature distribution in point D. $\omega = 710\ \text{RPM}, v = 40\ \text{mm/min}$

The modeling of this work is solved and the temperature distribution obtained for the model and the result show that there is good agreement between present work and ANSYS result. The difference in results of temperature distribution between experimental examination and modeling ranged between 5 – 14% which its acceptance.

Figures 17 to 24 show the maximum temperature of welding plate which has been reached at several time steps:

:

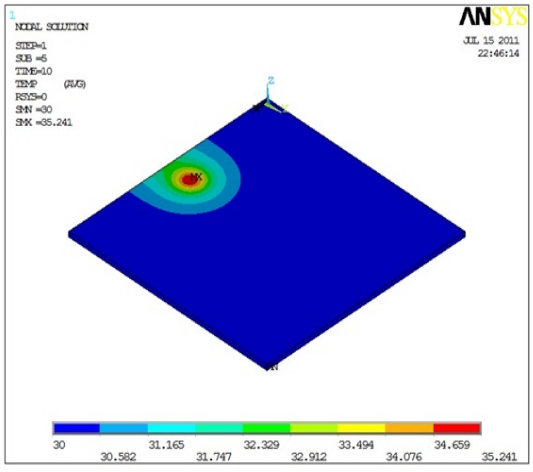

Fig. 17: Temperature distribution at 10 s, Max. Temp. 35 C^0

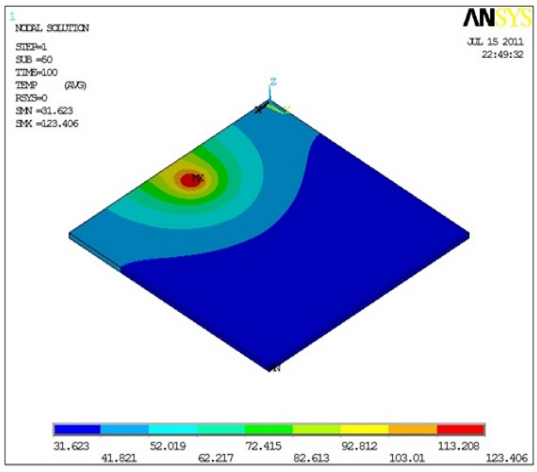

Fig. 18 :Temperature distribution at 100 s, Max. Temp. 123 C^0

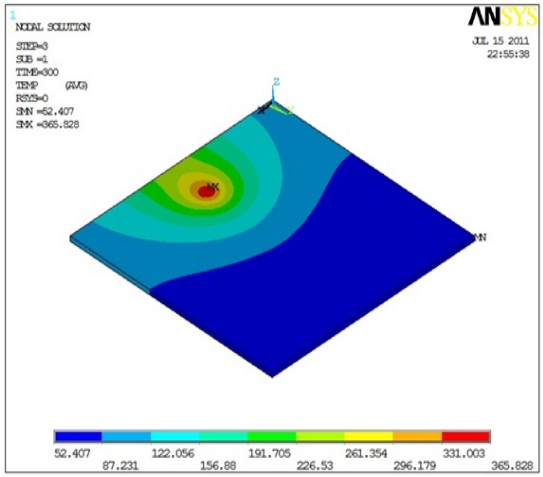

Fig. 19 :Temperature distribution at 300 s, Max. Temp. 365 C^0

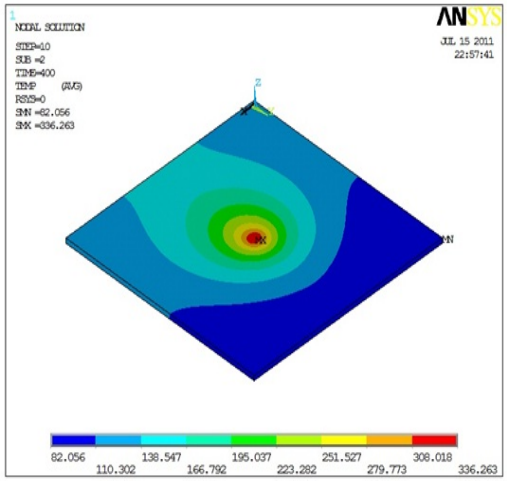

Fig. 20 :Temperature distribution at 400 s, Max. Temp. 336 C^0

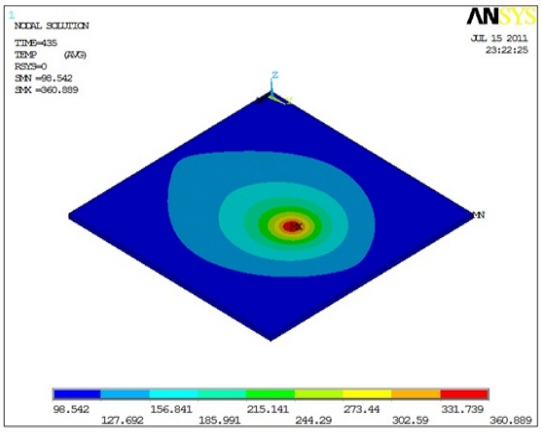

Fig. 21:Temperature distribution at 435 s, Max. Temp. 360 C^0

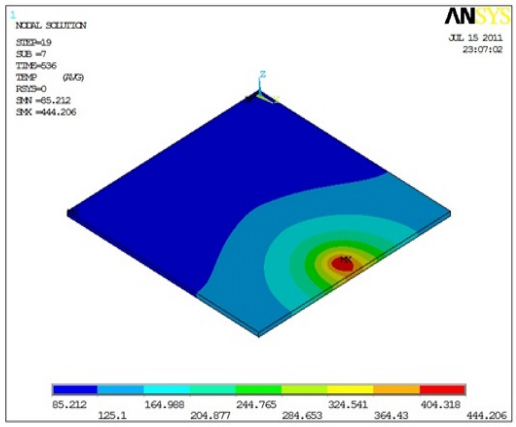

Fig. 22:Temperature distribution at 536 s, Max. Temp. 444 C^0

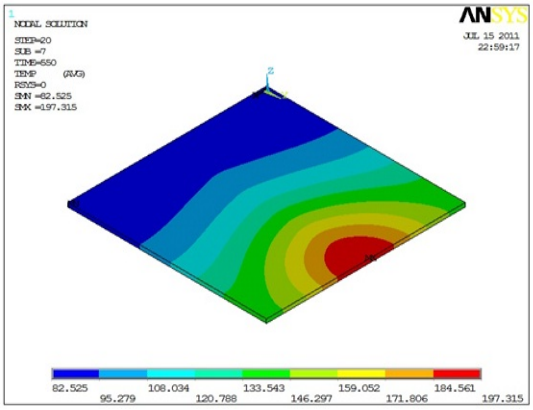

Fig. 23 : Temperature distribution at 550 s, Max. Temp. 197 C^0

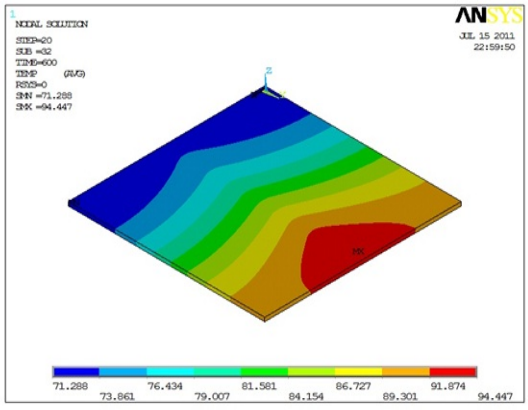

Fig. 24 : Temperature distribution at 600 s, Max. Temp. 94 C^0

As it is seen, temperature gradient increases in front of the tool comparing to its backside, i.e., the temperature profile extends further towards the welded region behind the moving tool.

Because of shoulder rotation, the material flow near the top surface is accelerated, and therefore, material deformation on the top surface next to the contact region is higher than the region at the bottom side. The material deformation has an important role on the formation of the weld zone profile in FSW operations [23].

The predicted maximum temperature is 444 C^0 in the region under the shoulder on the top surface. This temperature is about 58 C^0 below the solidus temperature of Al 2024 and is within accepted temperature range in FSW process.

Figures 13 to 16 shows the thermal cycles in the various points of sample No.6 at the depth of 1.5 mm. It can be seen that heating rate is higher than the corresponding cooling rate to room temperature.

As expected, the peak temperatures are higher at locations close to the weld line, and it decreases toward the HAZ.

Conclusion

1- Variation of the nugget-zone temperature with respect to time.

2- The temperature decreases with distance perpendicular direction of the tool on the top surface.

3- The variation of peak temperature with respect to thermal conductivity, specific heat and density is obtained.

4- Comparison of temperature profile developed between simulation values and the experimental results showed the possibility of more accurate determination using present simulation.

REFERENCES

1. **M. Awang, et. al.** "Experience on Friction Stir Welding and Friction Stir Spot Welding at Universiti teknologi petronas", journal of applied sience 11(2011):pp.1959-1965.

2. **M. Vural, et. al.** "On the Friction Stir Welding of Aluminium alloys EN AW 2024-0 and EN AW 5754-H22", Archives of Materials Science and Engineering, Volume 28, Issue 1,(2007),pp.49-54.

3. **S. Rajakumar, et. al.** "Statistical Analysis to Predict Grain Size and Hardness of the Weld Nugget of Friction-Stir-Welded AA6061-T6 aluminium alloy joints", Int J Adv Manuf Technol (2011) 57:151–165, DOI 10.1007/s00170-011-3279-5.

4. **Kevin Deplus, et. al.** "Residual Stresses in Aluminium Alloy Friction Stir Weld", Int J Adv Manuf Technol (2011) 56: pp.493–504.

5. **Ciro Bitondo, et. al**. "Friction-Stir Welding of AA 2198 butt joints: Mechanical Characterization of The Process and of The Welds Through DOE Analysis", Int J Adv Manuf Technol (2011) 53:pp.505–516.
6. **Mohammad Riahi & Hamidreza Nazari** "Analysis of Transient Temperature and Residual Thermal Stresses in Friction Stir Welding of Aluminum Alloy 6061-T6 via Numerical Simulation", Int J Adv Manuf Technol (2011) 55:pp.143–152.
7. **Dong-yang Yan, et. al.** "Predicting Residual Distortion of Aluminum Alloy Stiffened Sheet After Friction Stir Welding by Numerical Simulation", Materials and Design 32 (2011)pp. 2284–2291.
8. **P. Prasanna, et. al.** "Experimental and Numerical Evaluation of Friction Stirs Welding of AA 6061 –T6 Aluminum alloy", ARPN Journal of Engineering and Applied Sciences, VOL. 5, NO. 6,(2010).
9. **P. Prasanna, et. al.** "Finite Element Modeling for Maximum Temperature in Friction Stir Welding And Its Validation", Int J Adv Manuf Technol (2010) 51:pp.925–933.
10. **S. Mandal, et. al. "**The Effect of The Alclad Layer on Material Flow and Defect Formation During Friction-stir Welding", Metallurgical and Materials Transactions, Volume 42, Issue 6,(2011),pp.1717-1726.
11. **H. Jamshidi Aval, et. al.** "Experimental and Theoretical Valuations of Thermal Histories and Residual Stresses in Dissimilar Friction Stir Welding of AA5086-AA6061", Int J Adv Manuf Technol, (2011), DOI 10.1007/s00170-011-3713-8.
12. **H. Jamshidi Aval, et. al. "**Evolution of Microstructures and Mechanical Properties in Similar and Dissimilar Friction Stir Welding of AA5086 and AA6061", Materials Science and Engineering, Volume 528, Issue 28, pp.8071- 8083 (2011).
13. **Z. Zhang, et. al. "**Coupled Thermo-Mechanical Model Based Comparison of Friction Stir Welding Processes of AA2024-T3 in Different Thicknesses", J Mater Sci (2011) 46: pp5815–5821, DOI 10.1007/s10853-011-5537-1.
14. **Mohamed Assidi and Lionel Fourment** "Accurate 3d friction stir Welding Simulation Tool Based on Friction Model Calibration", Int J Mater Form Vol. 2 (2009) 1:327–330.
15. **G. Buffa, et. al.** "A new Friction Stir Welding Based Technique for Corner Fillet Joints: Experimental and Numerical Study", Int J Mater Form Vol. 3 (2010) 1:pp.1039 – 1042.

16. **Z. Zhang & H. W. Zhang** "Material Behaviors and Mechanical Features in Friction Stir Welding Process", Int J Adv Manuf Technol (2007) 35:pp.86–100.

17. **R. Palanivel, et. al.** "Development of Mathematical Model to Predict the Mechanical Properties of Friction Stir Welded AA6351 Aluminum Alloy", Journal of Engineering Science and Technology Review 4 (1) (2011)pp. 25-31.

18. **Manthan Malde** " Thermomechanical Modeling and Optimization of Friction Stir Welding" , B.E., Osmania University, Hyderabad, India,(2009).

19. **Ø. FRIGAARD, et. Al.** "A Process Model for Friction Stir Welding of Age Hardening Aluminum Alloys", Metallurgical and Materials Transactions a volume 32a, (2001), 1189-1200.

20. **Kenneth C Mills** "Recommended Values of Thermophysical Properties for Selected Commercial Alloys ", The Materials Information Society ***ASM,*** (2005).

21. **Vijay Soundararajan, et. al**. " Thermo-Mechanical Model With Adaptive Boundary Conditions for Friction Stir Welding of Al 6061", International Journal of Machine Tools & Manufacture 45 (2005) pp.1577–1587.

22. **R. Nandan, et. al**."Three-dimensional Heat and Material Flow During Friction Stir Welding of Mild Steel ", Acta Materialia 55 (2007)pp. 883–895.

23. **H. Jamshidi Aval, et. al.** "Theoretical and Experimental Investigation into Friction Stir Welding of AA 5086", Int J Adv Manuf Technol (2011) 52: pp.531–544.

24. **Myer Kutz** "Mechanical Engineering Handbook", Third edition, Material and Mechanical design, (2006).

25. **Hakan Aydin , et. al.**"Tensile Properties of Friction Stir Welded Joints of 2024 Alluminume Alloy in Different Heat Treated State", J Master design, doi:10.1016/j.matdes. (2008).08.034